The European Journal of Research and Development

journals.orclever.com/ejrnd

OR CLEVER Science & Research Group

Research Article

Numerical and Experimental Investigation of the Effects of Thermal Expansion and Pressure Loss in Air Hoses made from Different Materials

Aslıhan Çakır[1], Kemal Furkan Sökmen[2*]

[1] Bursa Technical University, Graduate School of Education, Orcid ID: 0000-0002-2631-744X, aslihancakiir@gmail.com

[2] Bursa Technical University, Faculty of Engineering and Natural Sciences, Department of Mechanical Engineering, Orcid ID: 0000-0001-8647-4861, furkan.sokmen@btu.edu.tr

[*] Correspondence: furkan.sokmen@btu.edu.tr; Tel.: (+90535641937)

(First received February 27, 2022 and in final form May 26, 2022)

Reference: Sökmen, K. F., & Çakır, A. . Numerical and Experimental Investigation of the Effects of Thermal Expansion and Pressure Loss in Air Hoses made from Different Materials. *The European Journal of Research and Development*, *2*(2), 383–399.

Abstract

This study was carried out to numerically and experimentally examine the thermal expansion of four different air hoses with the same geometric shape and dimensions, produced from rubber types with different raw materials, and to examine its effects on pressure loss. Hoses are manufactured from EPDM, ECO, AEM and NBR/CSM rubber compounds. The thermal expansion test was performed at 100°C and 140°C. Thermal and flow analyzes and solid-fluid interaction (FSI) analyzes were performed with ANSYS 19.2 commercial finite volumes software. In the study, independence from mesh number was studied. k- ε was chosen as the turbulence model. As a result of the study, the maximum expansion was observed in ECO material and in AEM, EPDM and NBR/CS materials, respectively. It has been determined by tests and analyzes that air hoses made of AEM and ECO materials with a low modulus of elasticity have the highest values in diameter expansion. These deformation values caused the pressure value of 300 kPa to decrease to 298.5 kPa at 100 °C and to 298.41 kPa at 140 °C for AEM and decreased the 300 kPa pressure value to 298.1 kPa for ECO. It has been determined that the importance of material selection in air hose designs and the deformation due to the material will affect the pressure loss.

Keywords: Thermal expansion, Air hose, Pressure loss, Fluid flow, Computational fluid dynamics, Fluid solid interface

1. Introduction

When objects or substances are exposed to heat, changes in their volume are observed. This is one of the characteristic features of objects or substances. Thermal expansion is the tendency of an object to change in volume under temperature change. Expansion and contraction are observed in railway tracks and bridges due to changing seasonal conditions. Expansion joints are used to prevent breakage or damage that may occur in these structures. [1]. Expansion joints allow volume changes to occur freely in response to temperature. In addition, these joints are equipment designed to absorb vibration on structures, hold certain parts together, allow movement due to ground settlement or earthquakes [1,2].

The expansion mechanism is related to molecular activity and interatomic bonds. When an object is heated, an increase in the kinetic energy of each atom occurs. This situation increases the molecular activity of the object and an increase in the energy stored in the bonds between atoms is observed. This increase in energy causes the molecular bonds to increase in length. A solid body is composed of atoms or molecules in a closer arrangement than gas and liquid bodies. The kinetic energy that increases in response to the heat occurring in the body atoms; transmit it to neighboring atoms or molecules in the form of small, fast vibrations. This causes the distance between atoms to increase as shown in Figure 1. For most substances under ordinary conditions, there is no preferred direction and an increase in temperature will increase the size of the solid at an inhomogeneous rate [3].

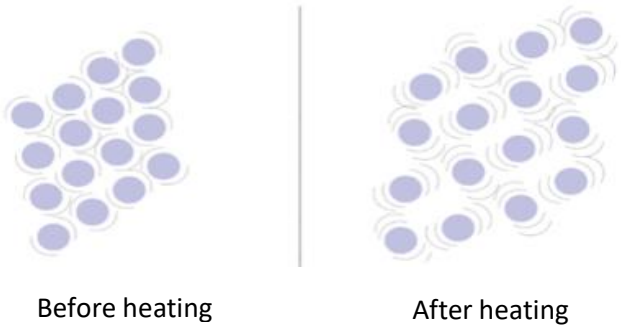

Figure 1 Expansion and contraction of particles

The coefficient of thermal expansion is a material property that indicates how much a material expands when heated. Each material expands by different amounts under the same temperature. In small temperature ranges, the thermal expansion of homogeneous materials is directly proportional to the temperature change [4]. It is a type of material that has the ability to return to its original state after force is applied to the rubber and removed. As the usage area; Many products such as tires, cables, hoses and clothes can be given as examples. In a report published in 2017; It has been stated that the total rubber

consumption worldwide increased by 1.8% in 2016 compared to the previous year and reached 27.2 million tons [5]. The most widely used rubbers; cis-polyisoprene (natural rubber, NR), ethylene propylene diene monomer (EPDM), acrylonitrile butadiene rubber (NBR), Ethylene acrylate copolymers (AEM), silicone rubber (SR), Epichlorohydrin rubber (ECO), Chlorosulfonated Polyethylene (CSM) and chloroprene rubber (CR) can be given as an example.

The properties of rubber products are not only dependent on the properties of the rubber raw material. In synthetic rubbers, various additives and components are present that are mixed into the raw material to form a rubber compound. These chemicals, binders, materials such as carbon black are added to the rubber in order to increase the mechanical properties of the rubber. Therefore, they directly affect the properties of rubber. The selection and inclusion of additives to improve the properties of raw materials depend on the industry, place of use and conditions of use of the rubber [6].

FSI; It can be expressed as fluid-structure interaction simulations. In these simulations; CFD (Computational Fluid Dynamics) and FEM (Finite Element Method) analyzes are examined together. FSI is highly dependent on CFD results for accuracy. Because the surface pressure information of the fluid for structural analysis is a result of CFD analysis [7].. FSI is the interplay between a deformable structure and an internal or surrounding fluid flow. The fluid to which the structure is exposed applies a pressure load that causes the structure to deform. FSI; automotive and aerospace industries (door seals, wings), biomechanical applications (design of heart valves), construction industry (wind loading of structures) etc. It is a very important type of analysis used in industrial applications [8].

Thermal expansion is an important phenomenon in many fields such as automotive, aviation, transportation, defense, food machinery, electronics. Wong & Bollampally, (1999) conducted a study on the thermal conductivity, elastic modulus and coefficient of thermal expansion of polymer composites filled with ceramic particles for electronic packaging. In the study, thermal conductivity, elastic modulus and thermal expansion coefficient of ceramic filled epoxy resins such as silica, alumina and aluminum nitride were determined. The thermal expansion coefficient of the samples was made on a Thermal Mechanical Analyzer (TMA) (TA Instruments, Model 2940) using an expansion probe. The result of the study showed that the relationship between the coefficients of thermal expansion is alumina, alumina nitride and silica, from largest to smallest, respectively [9].

In a study by Sleight, (1995)the behavior of anisotropic materials in the face of heat was investigated and the result was expressed as follows; It is expected that almost all materials expand as they are heated, because the interatomic distance between two bonded atoms generally increases with increasing temperature. The reason for this expansion in the study; It is expressed as that the energy required for the bonded atoms

to approach each other is greater than the energy required to repel each other. Therefore, vibrations of thermally excited atoms tend to perform motion that requires less energy. Therefore, an average increase in the interatomic distances is observed in reed conditions exposed to heat [10]. Sokmen & Karatas, (2020) determined in their study that there is a pressure loss due to thermal expansion in the air hose made of rubber material [11]. However, Sokmen and Karataş (2020) did not work on the difference in rubber material. In this study, the thermal expansion of 4 different rubber materials at two different temperatures was investigated and the pressure loss due to this expansion was investigated.

2. Materials and Methods

Turbulent flow is a very irregular fluid motion at high velocities characterized by velocity fluctuations. The transition from laminar to turbulent flow is not abrupt and an intermediate flow regime is experienced. As a result of rapid changes in turbulent flow, intense mixing of the fluid increases the momentum transfer between fluid particles. The Reynolds number at which the flow becomes turbulent is called the critical Reynolds number. The critical Reynolds number is different for different geometries and flow conditions. The generally accepted value of the critical Reynolds number for internal flow in a circular pipe is 2300. The Reynolds number is calculated according to Equation (1) [12].

$$Re = \frac{\rho VortD}{\mu} \quad (1)$$

In a common piping system, fluid passes through many fittings, valves, turns, elbows, tees, inlets, outlets, expansions and contractions, in addition to pipes. These elements interrupt the smooth flow of the fluid and cause additional losses as they separate the flow and cause flow mixing. In a system of long pipes, these losses are small compared to the total head loss (continuous head losses) in the pipes and are called local losses. The local losses are calculated according to the loss coefficient K_L Equation (2) ([12].

$$\boldsymbol{K_L = \frac{h_L}{V^2/2g}} \quad (2)$$

The total head loss, including the local losses, is calculated by Equation (3) [12].

$$\boldsymbol{h_{L,Total} = (f\frac{L}{D} + \sum K_L)\frac{V^2}{2g}} \quad (3)$$

f is the darcy friction factor and is calculated from the Colebrook Equation or the Moddy diagram [12].

Thermal expansion in objects with the effect of temperature has often been observed. It is observed that the change in the size of an object in a thermal expansion event is linearly proportional to the change in the temperature of the object. This is the case where the temperature variation is not very large. This linear relationship is expressed in Equation (4) [13].

$$\Delta L = L_i \, \alpha . \Delta T \quad (4)$$

The final length of the object undergoing expansion; As in Equation (5), it is the sum of the initial size and length change of the object [13].

$$L = L_i + \Delta L = L_i + L_i \, \alpha . \Delta T = L_i \, (1 + \alpha . \Delta T) \quad (5)$$

L= Final length [mm]
L_i= Initial length [mm]
α= Thermal expansion coefficient [$°C^{-1}$]
ΔL= The amount of change in length [mm]
ΔT= The amount of change in temperature [°C]

If the object has a certain width (W) and height (H), the change in the field of the object and the new area can be expressed as Equation (6).

$$A = H.W = H_i . (1 + \alpha . \Delta T) . (1 + \alpha . \Delta T) = H_i . W_i . (1 + \alpha . \Delta T) . (1 + \alpha . \Delta T) = A_i . [1 + 2 \, \alpha . \Delta T + (\alpha . \Delta T)^2] \quad (6)$$

For materials with very small coefficient of thermal expansion, the value of $\alpha.\Delta T$ decreases significantly in Equation 1, so the term $(\alpha.\Delta T)^2$ can be neglected compared to the term $2\alpha.\Delta T$. The areal change is as expressed in Equation (7) [13].

$$A = A_i . [1 + 2 . \alpha . \Delta T] \quad (7)$$

The amount of volumetric expansion can be obtained in a similar way to areal expansion. This change is noted in Equation (8) [13].

$$V = V_i . [1 + 3 . \alpha . \Delta T] \quad (8)$$

2.1. CFD Analysis

Computational Fluid Dynamics (CFD) is a numerical solution technique used to solve the viscous fluid-dynamic equation. Today's computing power can solve a wide variety of problems using CFD. As part of the CFD design process, it is used to quickly discover changes in geometry and see how changes affect resistance and thrust properties. In this study, the Ansys Fluent v.19.2 software was used to determine the pressure loss inside the hose. Mass, momentum and energy conservation equations were primarily solved in the analysis [14]. The Navier-Stokes equations, which are equations used to identify motions of fluids such as liquids and gases, were used to solve the equation. The incompressible version of the equation expressed by [12] is as Equation (9)

$$p\frac{D\vec{V}}{Dt} = -\vec{\nabla}p + \rho\,\vec{g} + \mu.\nabla^2\vec{V} \quad (9)$$

2.2.FEA Analysis

The Finite Element Method (FEM) is a widely used tool for performing calculations on structures and focusing on structural problems. It is based on finite element analysis (FEA) and is a very efficient method that gives excellent results for power calculations. Due to the developments in computer science and the capacity of modern computers, FEM is widely used by people from all walks of life due to its robustness, proven capabilities and accuracy, but experience and knowledge on the subject are very important to verify the final result. The finite element method is a numerical solution technique used to solve the approximation of a partial differential equation to the boundary value problem. The method divides the structure into a limited number of elements and aims to minimize an error function called residual [15]. Fish and Belytschko (2007) stresses in his study; It is expressed depending on the displacements (u) in the structure. The expression changes depending on what type of elements and formulations are used. In a one-dimensional bar element, the relationship is as follows Equation (10) [16]:

$$\varepsilon_{xx} = \frac{\partial U_X}{\partial X} \quad (10)$$

Here; U_x = Displacement in the x direction, ε_{xx} = Strain in the x direction. Matrix form in two-dimensional structures is given Equation (11) [16];

$$\varepsilon = \begin{bmatrix} \varepsilon_{xx} \\ \varepsilon_{yy} \\ \gamma_{xy} \end{bmatrix} = \nabla s.u = \nabla s \begin{bmatrix} U_x \\ U_y \end{bmatrix} \quad (11)$$

Here; γ_{xy}= shear stress

$$\nabla s = \begin{bmatrix} \frac{\partial}{\partial x} & 0 \\ 0 & \frac{\partial}{\partial y} \\ \frac{\partial}{\partial y} & \frac{\partial}{\partial x} \end{bmatrix} \quad (12)$$

There is a balance in all parts of a structure. Based on the equilibrium of a finite element with respect to internal forces (stresses) and external forces, the following Equation (13) can be studied:

$$\nabla s^T.\sigma + b = 0 \quad (13)$$

Here; $\nabla_s{}^T$=Transpose matrix, b= Vector of forces, σ= stress [16].

2.3.FSI Analysis

Fluid-Structure Interaction (FSI) is the analysis method used when there is a mutual interaction between a liquid-solid boundary and a gas-solid boundary. In this type of analysis, there is a match between the two domains, and to obtain satisfactory results, the problem must be solved with the paired shape of the interacting domains. The fluid affects the structure through compressive forces and the structure affects the fluid through structural deformations. Fluid-structure interaction analysis can be applied to a variety of problems. The main examples of these applications are; automotive industry, construction industry, transportation industry, healthcare industry (artificial heart valves), parachuting or analysis of wind turbines [17]. In a general FSI analysis, the behavior of the fluid is solved by CFD calculations, and the behavior of the solid is solved by FEA calculations. These two solution areas form the basis for computational fluid structure interaction analysis [15].

3. Experimental Methot

The hoses examined in the study are the hoses used in real conditions, located between the engine and the EGR cooler in automobiles. EGR cooler; It is used as exhaust gas recirculation in internal combustion engines and its purpose is to reduce nitrogen oxide (NOx) emissions used in engines. EGR works by returning some of an engine's exhaust gas back to the engine cylinders. Hoses are air hoses and are part of the system. The location of the hoses on the vehicle is given on the original technical drawing as follows Figure 2.

a) b)

Figure 2 a) *Location where hoses are used on the vehicle b) Air hoses used in this stud*

The operating range of the measuring device used in the tests is 0-40 bar for the pressure parameter and 0-150°C for the temperature parameter. The device sensitivity is ±0.01 bar and ±0.1°C.

Figure 3 Diameter expansion testing device.

The tests were performed at two different temperatures for four different types of rubber hose in test device (Figure 3 a). While one EPDM, ECO, AEM and NBR/CSM hoses, called the first group, were tested at 100°C, one EPDM, ECO, AEM and NBR/CSM hoses forming the second group were tested at 140°C. This allows us to examine the diameter expansion of different rubber hoses at the same temperature and the diameter expansion of the same rubber type at two different temperatures.

Before connecting the hoses to the device, the cabinet was heated to 100°C. The purpose of this is to prevent a heat transfer that may occur between the cabinet and the hose by bringing the internal and external temperature of the hose to the same level. To the hose; Two plugs are mounted on both ends with screw clamps. These plugs ensure that the fluid transfer is leak-free when connecting the hose to the device (Figure 3 b). Before the test starts, the initial diameter of the produced hose must be measured. With

the help of a thread, the outer circumference of the hose was measured and recorded. This method was defined in OEM specifications and was preferred in the study because it is practical and cost-effective. In this method, the yarn is tied to the outside of the hose as a single layer and the junction points of the yarns are marked. Then the intervals between these marks are measured. Thus, the circumference of the hose before thermal expansion and accordingly its initial diameter is determined. The hose whose initial diameter is noted is connected to the diameter expansion tester for thermal expansion. The required parameters are determined by the relevant OEM specification. According to the specification; hose pressure is increased by 1 bar per minute up to 3 bar. The hose is kept at maximum pressure (3 bar) for 30 seconds before being measured. When the test is completed, the circumference of the hose is measured with the same method, without removing the hose from the cabinet. The final environmental value obtained is saved in the program interface. The device program automatically calculates the diameter increase as a percentage using two circumference values. Since the hoses are of circular structure, the percentage of increase in the circumference of the hoses and the percentage of increase in the diameter of the hoses represent the same value.

The same processes are repeated for the other rubber types ECO, AEM and NBR/CSM hoses at 100°C. Then, the cabin and fluid temperature were heated to 140°C and the test was repeated for EPDM, ECO, AEM and NBR/CSM hoses. After each test device cover is opened, the cabinet is reheated to test temperatures (100°C and 140°C) in order to eliminate the heat loss in the cabinet. Thus, any heat transfer between the cabinet and the hose is prevented. The analyzes made in the study were carried out in the Ansys 19.2 program. Hose model focused in the study; It has a length of 181.4 mm, an inner diameter of 16.5 mm and a wall thickness of 3.5 mm (Figure 4).

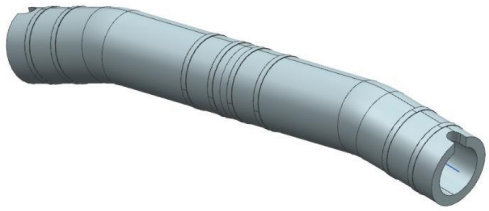

Figure 4: Geometric model of the hose

A tensile test was carried out to determine the mechanical properties of the hoses. In order to prepare the drawbar, the dimensions in the standards were used. Tensile test samples for each material are given in Figure 5a. These samples are prepared by cutting over the hoses in order to reflect the rubber material and the braid layer exactly. The dimensions of the tensile sample are given in Figure 5b.

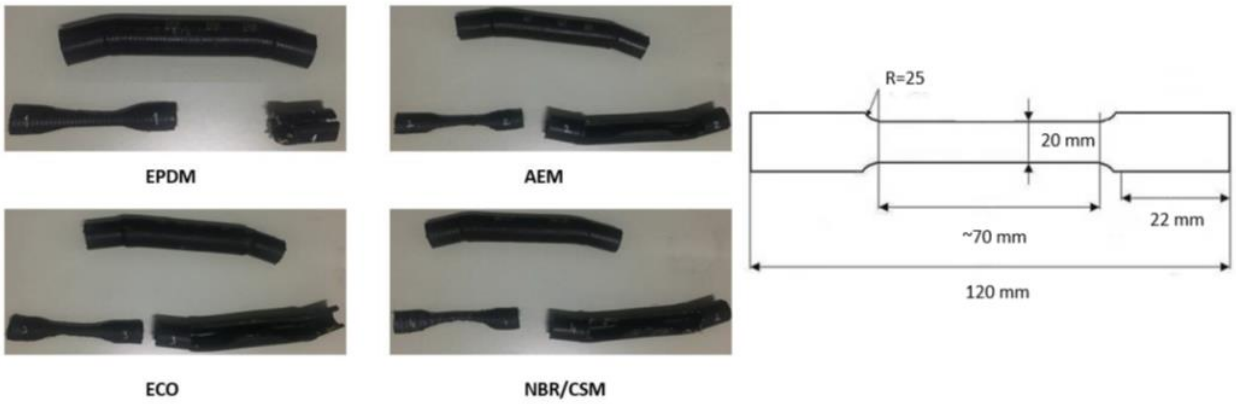

Figure 51: a) Tensile specimens cut through the hose. b) Dimensions of the tensile sample

Tensile test was carried out in Bursa Technical University Mechanical Engineering Laboratory. The device in the laboratory is a Shimadzu branded AG-XPLUS250KN AG model 250 kN mechanical test device (Figure 6). The test device is connected to a computer in order to enter the parameters and follow the test on the graph.

Figure 6.: Shimadzu branded AG-XPLUS250KN AG

The tensile test was carried out at a speed of 0.5 m/s. The test was carried out in a hose produced from four different types of rubber under the same conditions. The stress-strain graph created as a result of the tensile test of the samples cut from four different rubber hoses is given below.

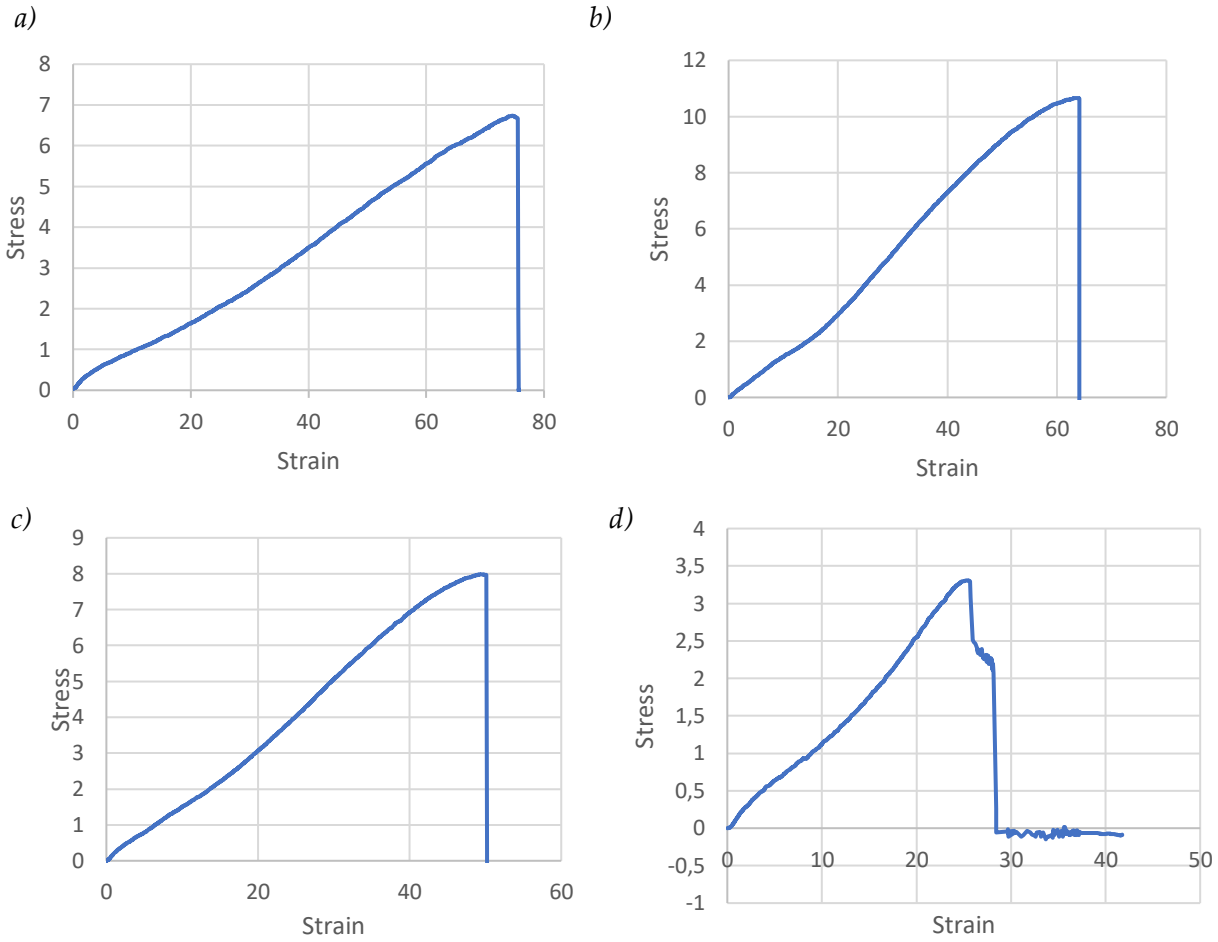

Figure 72: Kauçuk türüne ait gerilme-gerinim grafiği a) EPDM b) AEM c) ECO d) NBR / CS

The elasticity values obtained according to the stress and strain values taken from the elastic regions of the graphics are given in Table 1.

Table 1. Modulus of elasticity by rubber type.

Rubber Type	E [MPa]
EPDM	10,866
AEM	6,237
ECO	5,795
NBR/CSM	11,165

The initial conditions of the analysis are listed in Table 2.

Table 2. Initial conditions of analysis at 100°C and 140°C.

Initial Conditions	Inlet	Outlet
Temperature	100°C ve 140°C	
Pressure	300 kPa	-
Mass Flow	-	300 kg/h
Turbulance model	k-Ɛ	

The Reynolds number was calculated as 3.3 x 10^5. Therefore, the flow is turbulent. The k-Ɛ turbulence model was used in the analysis. The k-Ɛ turbulance has been used because of its extensive use in the literature and because it gives validated results in its use in solid channel flows. The boundary conditions were given to in Table 3. The convergence criterion was assumed 10^{-3} similar to the study [16].

In terms of the accuracy of the analysis, the number of elements should be chosen optimally. For this reason, it is preferred that the number of elements and the mesh structure be optimum. In the study, the independence study from the element number was made. The minimum number of elements for CFD analyzes was chosen as at least 253561 and for finite element analysis at least 970841. CFD element structure in Figure 8a. Finite element mesh structure is given in Figure 8b.

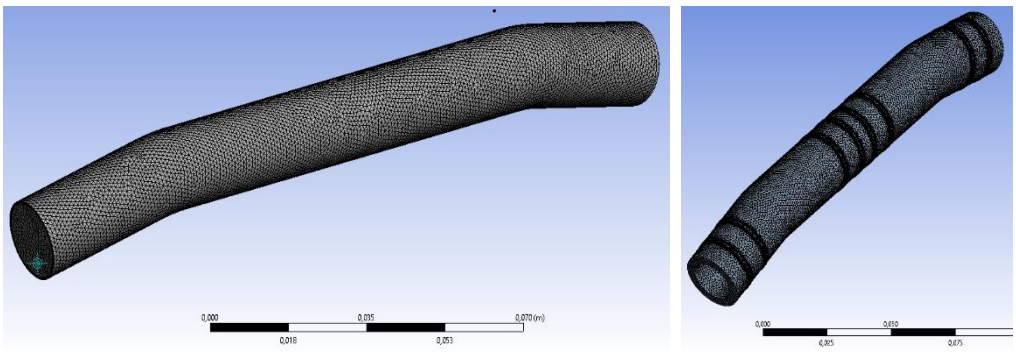

a) *b)*

Figure 83: a) CFD mesh b) FEM mesh

The results of the analyzes made under two different temperature values were exported to be used in the Ansys program. The results of the CFD analysis are important for static analysis as well as for comparing the maximum pressure after the diameter expansion test and confirming the accuracy of the test and analysis.

4. Results

CFD analysis is important in terms of providing preliminary information to the next step, structural analysis. Pressure distribution is important in predicting which areas the hose will expand. Pressure distribution obtained from CFD analysis at 100°C and 140°C is given in Figure 9-1.

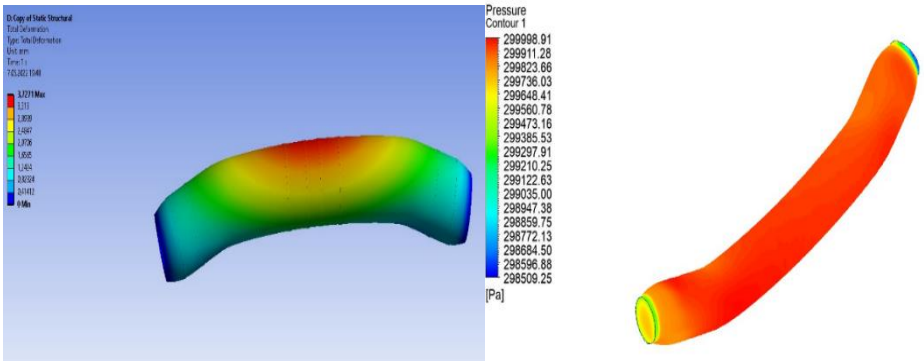

a)

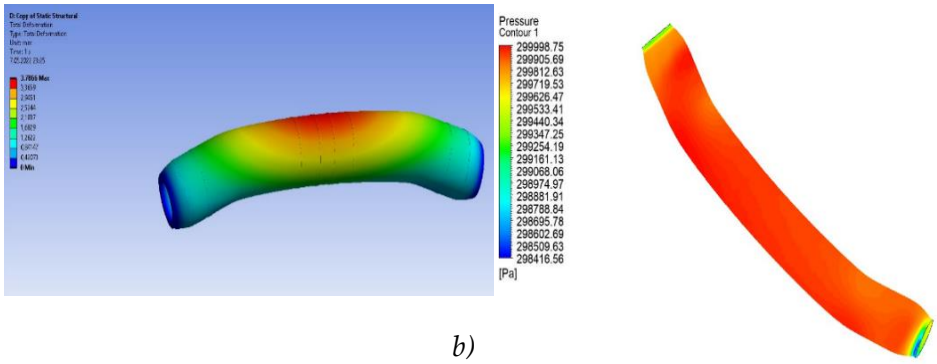

b)

Figure 9: AEM deformation and pressure lost a) 100 °C b) 140 °C

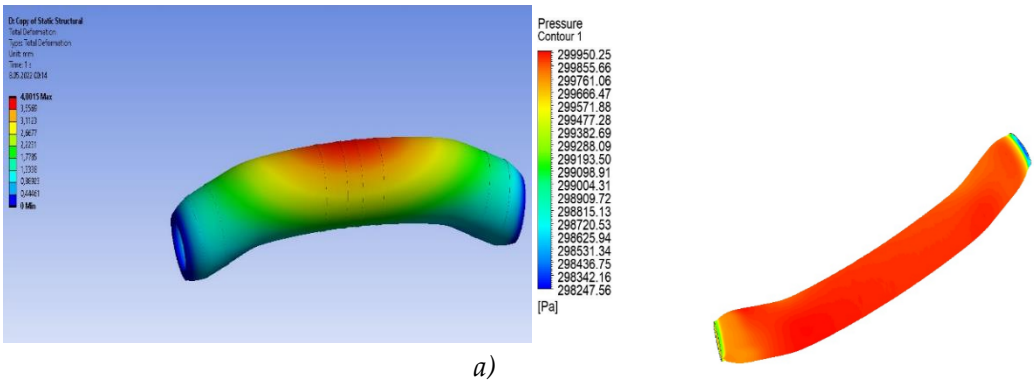

a)

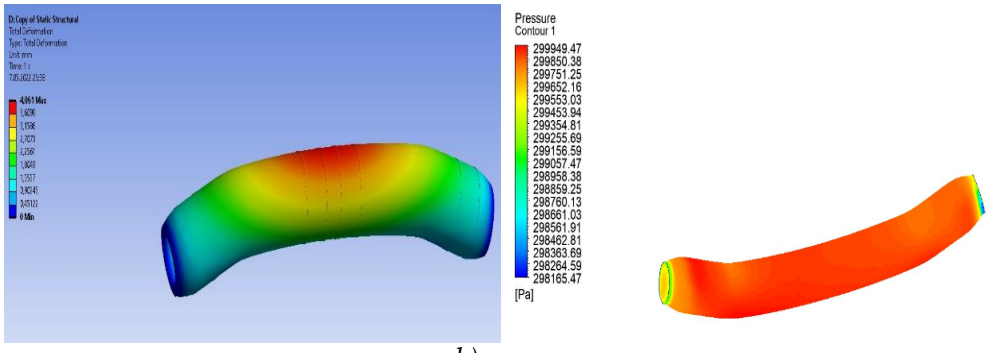

b)

Figure 10: ECO deformation and pressure lost a) 100 °C b) 140 °C

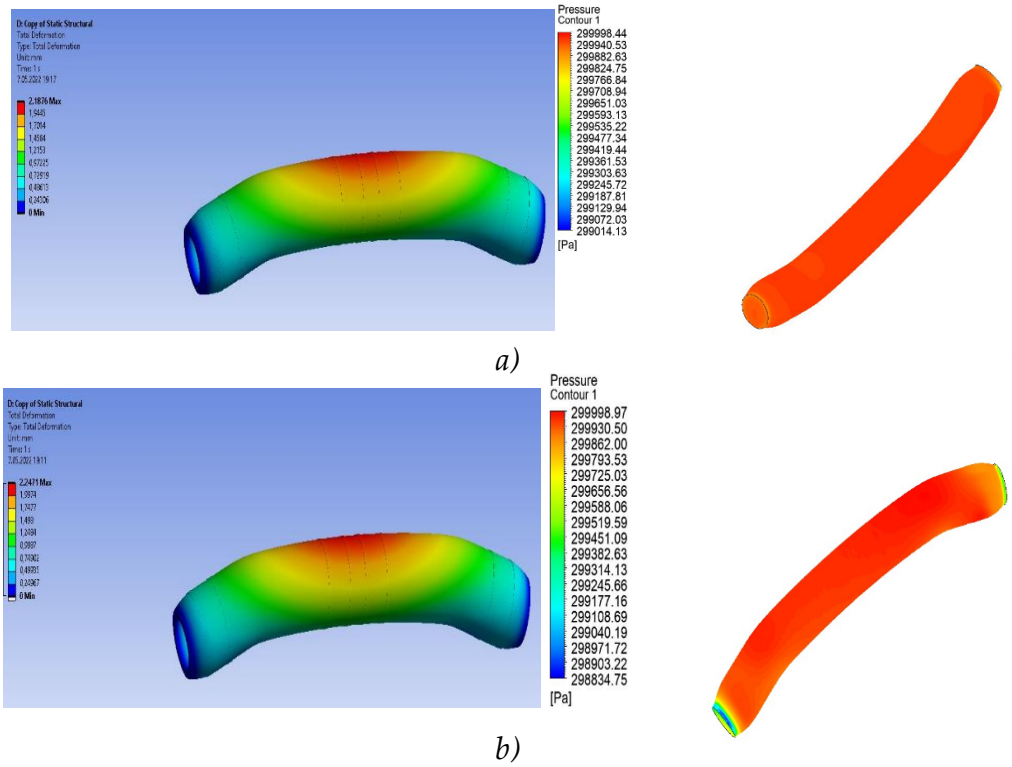

Figure 11: EPDM deformation and pressure lost a) 100 °C b) 140 °C

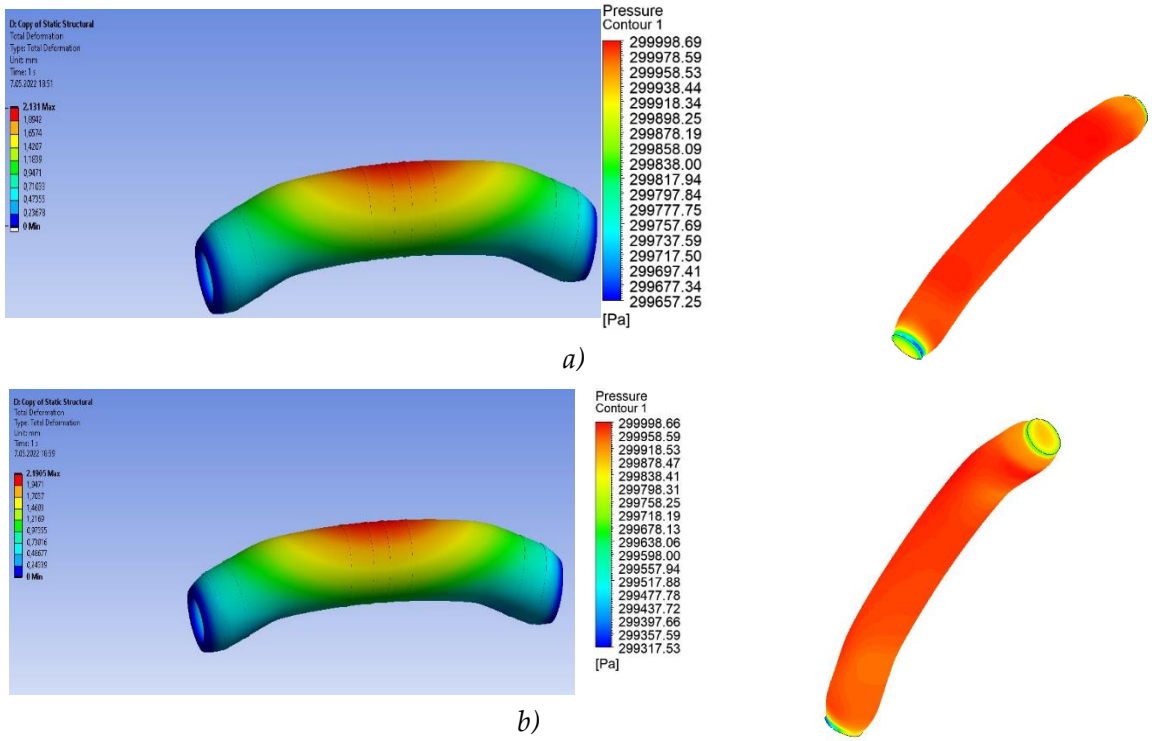

Figure 12: NBR deformation and pressure lost a) 100 °C b) 140 °C

The fluid is exposed to various pressure losses from the moment it enters the pipe to the moment it exits. These pressure losses; The friction forces in the opposite direction to the flow are the losses that occur in diameter changes, in areas with radius, in areas with sudden diameter contractions and expansions, in parts where there are connection elements such as valves and pumps [19].. The tests were simulated with the help of Ansys analysis programs and the results were shown in Table 5. It is listed in the chart in 5. This chart represents the results of the diameter expansion test and thermal expansion analysis at 100°C. The results of the diameter expansion test and thermal expansion analysis performed at 140°C are given in Table 6:

Table 3. Diameter expansion test and thermal expansion analysis results at 100°C.

Rubber Type	Diameter Expansion Test Result [mm]	Thermal Expansion Analysis Result [mm]
EPDM	2,04	2,18
AEM	3,65	3,72
ECO	3,86	4
NBR/CSM	2,01	2,13

Table 4. Diameter expansion test and thermal expansion analysis results at 140°C.

Rubber Type	Diameter Expansion Test Result [mm]	Thermal Expansion Analysis Result [mm]
EPDM	2,18	2,24
AEM	3,59	3,78
ECO	3,98	4,06
NBR/CSM	2,08	2,19

5. Discussion and Conclusion

In the examination made for four rubber types at 100°C and 140°C, it was determined that the ECO rubber type was the rubber type with the highest expansion. Afterwards, AEM, EPDM and NBR\CSM hoses come, respectively, according to their expansion amounts. The deformation values of EPDM and NBR/CSM materials obtained at 100 °C and 140 °C are between 2.13-2.2 mm. It has been determined that these diameter expansion values do not affect the pressure loss much. It has been determined by tests and analyzes that air hoses made of AEM and ECO materials with a low modulus of elasticity have the highest values in diameter expansion. The diameter change value for AEM material is 3.72 mm at 100 °C and 3.78 mm at 140 °C. These deformation values

caused the pressure value of 300 kPa to decrease to 298.5 kPa at 100 °C and to 298.41 kPa at 140 °C. The ECO material expanded 4 mm at 100 °C and 4.06 mm at 140 °C. It was determined that these deformation values decreased the 300 kPa pressure value to 298.1 kPa.. In the study, it was revealed that the expansion values of the same rubber type at different temperature values depend on the elastic modulus of the material, especially materials with low modulus of elasticity such as AEM and ECO will increase the pressure loss at different temperatures. According to the study of Sokmen and Karataş (2020), it has been confirmed in this study that geometric deformation causes pressure loss in air hoses. In addition, this study revealed that the selection of materials used in air hoses should be made carefully, as this deformation depends on the material properties. This is the most important parameter for rubber selection. As can be seen from the results obtained, hoses tend to expand even at lower temperatures, which do not reach temperatures where their chemical structure is completely destroyed. This indicates that the modeling of hoses as fixed diameter solids in design and analysis is not correct and the calculations using this modeling do not reflect the worst-case scenario in the operating conditions of the hoses. Calculations that are not made according to the worst-case scenario are an indication that unexpected situations may be encountered.

6. Acknowledge

This study is produced from Aslıhan Çakır's Master's thesis under the supervision of Assist. Prof.Dr. Kemal Furkan SÖKMEN.

References

[1]. Çakır, A. (2019). *THERMAL EXPANSION ANALYSIS OF AIR HOSES PRODUCED FROM DIFFERENT ELASTIC MATERIALS*. Bursa Technical University

[2].Expansion Joints - SolidsWiki. (n.d.). Retrieved May 30, 2022, from http://www.solidswiki.com/index.php?title=Expansion_Joints.

[3]. Introduction to Thermal Expansion - Bright Hub Engineering. (n.d.). Retrieved May 30, 2022, from https://www.brighthubengineering.com/thermodynamics/20956-the-mystery-of-thermal-expansion/.

[4]. ASM International. (2002). Thermal Properties of Metals. *ASM Ready Reference*, 5–7.

[5]. Rubber Asia. (2017). Retrieved April 23, 2019, from https://www.rubberasia.com/2017/04/05/world-rubber-consumption-1-8-2016-says%02irsg/.

[6]. Thomas, S., Rane, A. V., Abitha, V. K., Kanny, K., Dutta, A. (n.d.). *Hydraulic Rubber Dam: An Effective Water Management Technology.*

[7]. Lee, K., Huque, Z., Kommalapati, R., & Han, S. E. (2017). Fluid-structure interaction analysis of NREL phase VI wind turbine: Aerodynamic force evaluation and structural analysis using FSI analysis. *Renewable Energy*, *113*, 512–531. https://doi.org/10.1016/j.renene.2017.02.071

[8]. Ezkurra, M., Esnaola, J. A., Etxeberria, U., Lertxundi, U., Colomo, L., Begiristain, M., & Zurutuza, I. (2018). Analysis of One-Way and Two-Way FSI Approaches to Characterise the Flow Regime and the Mechanical Behaviour during Closing Manoeuvring Operation of a Butterfly Valve. *International Journal of Mechanical and Materials Engineering*, *12*(4), 409–415.

[9]. Wong, C. P., & Bollampally, R. S. (1999). Thermal conductivity, elastic modulus, and coefficient of thermal expansion of polymer composites filled with ceramic particles for electronic packaging. *Journal of Applied Polymer Science*, *74*(14), 3396–3403. https://doi.org/10.1002/(SICI)1097-4628(19991227)74:14<3396::AID-APP13>3.0.CO;2-3.

[10]. Sleight, A. W. (1995). Thermal contraction. *Endeavour*, *19*(2), 64–68. https://doi.org/10.1016/0160-9327(95)93586-4.

[11]. Sokmen, K. F., & Karatas, O. B. (2020). Investigation of air flow characteristics in air intake hoses using CFD and experimental analysis based on deformation of rubber hose geometry. *Journal of Applied Fluid Mechanics*, *13*(3), 871–880. https://doi.org/10.29252/JAFM.13.03.30497.

[12]. Yunus A. Cengel, J. M. C. (n.d.). Akışkanlar Mekaniği (Temelleri ve Uygulamaları). Retrieved May 30, 2022, from https://palmeyayinevi.com/akiskanlar-mekanigi-temelleri-ve-uygulamalari-2-2-.

[13]. Andrew R. (2017). Thermal Physics: A Macroscopic View. Retrieved from http://www.webassign.net/question_assets/buelemphys1/chapter13/section13dash2.pdf.

[14]. Ansys Fluent Theory Guide. (2021). Ansys Fluent Theory Guide. *ANSYS Inc., USA*, *15317*(November), 724–746. Retrieved from http://scholar.google.com/scholar?hl=en&btnG=Search&q=intitle:ANSYS+FLUENT+Theory+Guide#0.

[15]. Handeland, M. P. (2015). Importance of Fluid-Structure Interaction on Dropped Lifeboats-A parametric study used to explore the importance of hydroelasticity on complex low rigidity structures using decision factors.

[16]. Fish, J., & Belytschko, T. (2007). *A First Course in Finite Elements*. *A First Course in Finite Elements*. John Wiley and Sons. https://doi.org/10.1002/9780470510858.

[17]. Zienkiewicz, O.C., R. L. T. and P. N. (2014). *The Finite Element Method for Fluid Dynamics*.

[18]. Kumar, J. S., & Ganesan, V. (2004). Flow through S.I. engine air intake system using CFD at part throttle and full throttle. *Indian Journal of Engineering and Materials Sciences*, *11*(2), 93–99.

[19]. Aracı, S., & Kınacı, Ö. K. (2018). Boru İçi Akışlarda Basınç Kaybının Sayısal Hesabı Numerical Analysis of Pressure Loss in Pipe Flow, (March), 38–59.